Advanced characterization of albumin adsorption on a chemically treated surface for osseointegration: An innovative experimental approach

Materials & Design 218 (2022) 110712

Contents lists available at ScienceDirect

Materials & Design

journal homepage: www.elsevier.com/locate/matdes

Advanced characterization of albumin adsorption on a chemically treated surface for osseointegration: An innovative experimental approach

Jacopo Barberi [a,*], Sara Ferraris [a], Andrea Mario Giovannozzi [b], Luisa Mandrile [b], Erik Piatti [a], Andrea Mario Rossi [b], Silvia Spriano [a]

[a] Department of Applied Science and Technology, Politecnico di Torino, Corso Duca degli Abruzzi 24, 10129 Torino, Italy
[b] Chemical physics and nanotechnology department, National Institute of Metrological Research, Strada delle Cacce 91, 10137 Torino, Italy

HIGHLIGHTS

- Characterization techniques are need for study protein adsorption on rough biomaterials.
- Albumin adsorption is investigated on polished and surface modified Ti6Al4V by new methods.
- Kelvin probe force microscopy allows imaging of the adsorbed protein layer.
- Protein structure was studied by surface enhanced Raman scattering and ζ potential.
- OH surface groups density determines the amount and conformation of protein adsorbed.

GRAPHICAL ABSTRACT

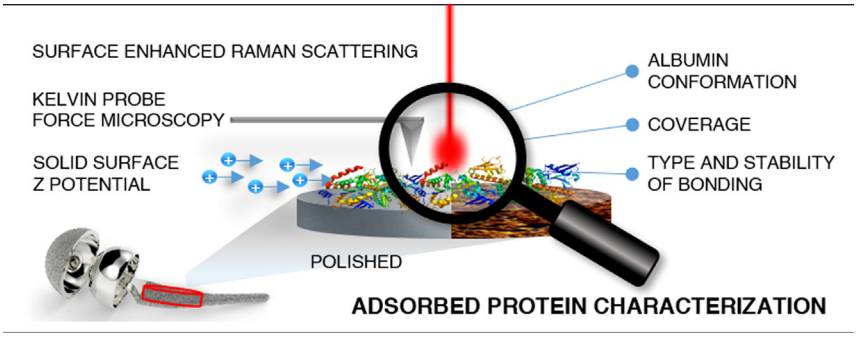

ARTICLE INFO

Article history:
Received 8 February 2022
Revised 28 April 2022
Accepted 28 April 2022
Available online 04 May 2022

Keywords:
Surface Enhanced Raman Scattering
Surface analysis
Protein adsorption
Titanium
Zeta potential
Kelvin-probe force microscopy

ABSTRACT

Surface chemistry, charge, wettability, and roughness affect the adsorbed protein layer, influencing biocompatibility and functionality of implants. Material engineering seeks innovative, sensitive, and reliable characterization techniques for study the adsorbed proteins. These techniques must be suitable to be directly used on the surfaces of clinical interest. In this paper, the characterization of surfaces with topography and chemistry developed for osseointegration is performed by innovative surface analysis techniques to investigate the properties of adsorbed bovine serum albumin. Ti6Al4V alloy chemically treated with an oxidative process to obtain peculiar surface features (roughness and surface hydroxylation) was tested and compared with mirror-polished titanium. Albumin forms a continuous layer on both Ti surfaces when adsorbed from near physiological concentrations, as proved by Kelvin force probe microscopy. It was observed that the hydroxylation degree plays a pivotal role in determining the conformation of proteins after adsorption, where it strongly drives protein unfolding, as confirmed by Surface Enhanced Raman scattering, and in influencing the mechanism and chemical stability of protein-surface interactions, which was highlighted by zeta potential titration curves.

1. Introduction

Evolution of metal implants progressively shifted the focus from adequate mechanical strength to improved biocompatibility

* Corresponding author.
E-mail address: jacopo.barberi@polito.it (J. Barberi).

https://doi.org/10.1016/j.matdes.2022.110712
0264-1275/

and, finally, to multifunctional surfaces, such as osteogenic and antibacterial [1]. In particular, the current clinical demand requires multifunctional surfaces for bone contact able to achieve fast osseointegration in critical patients, with sealing adhesion of soft tissues to avoid bacterial infiltration (in case of transcutaneous or transmucosal implants), with tailorable active antibacterial action, and modulation of the inflammatory response [2]. This evolution was achieved by different material engineering approaches such as deposition of thick and thin inorganic coatings [3], chemical surface treatments [4], or growth of nanostructures such as nanotubes by surface anodization [5] and finally surface functionalization/-coating with biomolecules or drugs [1]. The goal is to achieve tailored surface roughness (both at the micro- and nano-scale) and chemistry for such a multifunctional behavior [6].

One of the crucial aspects to achieve effective biomaterials, lies in the possibility to tailor adsorption of proteins, to elicit an appropriate cellular response. To attain this purpose, it is necessary to deepen the knowledge on adsorption of proteins on surfaces for osseointegration, which is not fully understood due to the complexity of the phenomenon [7]. The formation of a protein layer takes place within minutes since implantation and it mediates the further interaction of the surface with the cells [8]. Many surface properties, such as surface chemistry, charge, wettability, and roughness affect not only the amount of the adsorbed proteins, but also the type of bond created with the surface and conformation of the adsorbed proteins [9]. Specifically, the inflammatory response, which is a crucial phase for the good success of an implant, and should always be maintained under control, is mediated by protein adsorption on the implant surface [10]. The presence of anti-inflammatory proteins within the adsorbed layer, such as albumin, can reduce the long term inflammation processes [11]. As an example, downregulation of pro-inflammatory cytokines was registered on hydrophilic-modified Ti surfaces [12].

Specific sensitive techniques for surface characterization, suitable to be applied on a wide variety of biomaterials in terms of surface chemistry and roughness, are of primary importance for this purpose. Currently, investigation of adsorption on mirror-polished model surfaces can be performed through several techniques (such as spectroscopic ellipsometry and quartz crystal microbalance, QCM), but there is a lack of characterization techniques suitable for the real implant surfaces which are usually rough at the micro-scale and present non-standard surface composition. For instance, even though titanium coated QCM sensors have been used for adsorption studies [13,14], such surfaces cannot withstand common surface modification treatments for titanium implants, such sandblasting or chemical treatments. In this paper, three innovative surface analysis techniques were applied for the characterization of the adsorption of a model protein (i.e. bovine serum albumin, BSA) on Ti alloys alternatively polished or chemically treated with an oxidative process to obtain surface features (roughness and surface hydroxylation) suitable for osseointegration: Kelvin Probe Force Microscopy, Surface Enhanced Raman Scattering and Zeta Potential titration curves.

Kelvin probe force microscopy (KPFM) is a measurement method for atomic force microscopy (AFM) which allows measuring the surface potential, or work function, of a surface and to compare topographical and surface potential images [15]. KPFM has been used mainly for the characterization of electrical properties at the nanoscale of semiconductor devices and conductive/semiconductive surfaces [15]. Recently, this technique has been applied also to investigate biomaterials, biological materials and molecules, such as polymeric fibers for tissue integration [16,17] DNA nanoarrays [18], oligonucleotides, and amyloid fibrils [19]. In the last few years, KPFM was also used to investigate protein adsorption on mirror polished Ti6Al4V and CoCrMo alloy, under different conditions of protein solution and surface polarization [20,21]. In this work, we observed that KPFM is a valuable method to image the layer formed by albumin on a rough substrate suitable for osseointegration.

Compared to other analytical techniques, vibrational spectroscopy (including infrared (IR) absorption spectroscopy and Raman spectroscopy, RS) allows fast and label-free detection of molecular targets, high selectivity due to the specific vibrational fingerprint of molecules, and minimal or no preliminary treatment of the sample [22,23]. In addition, RS has great potential for surface analysis. In particular, the sensitivity of normal RS, which may not be sufficient to detect a layer of proteins adsorbed on a biosurface, can be increased by several orders of magnitude by Surface Enhanced Raman Scattering (SERS) thanks to the enhancement of the Raman scattering of molecules adsorbed onto, or microscopically close to, a suitable plasmonically-active surface, such as metal nanoparticles [24,25]. For all these reasons, SERS represents a good candidate for surface analysis of very thin films. Gold nanostars and thin films were used to develop SERS-active substrates in order to investigate protein interactions with chemically modified surfaces [26] or protein–protein interactions such as aggregation [27]. However, even though these SERS substrates demonstrated a very high sensitivity in protein analysis, they usually suffer from lack of applicability for direct investigation of biomaterials for real use. In this work, we propose a versatile and simple SERS method by drop casting of silver nanoparticles (AgNPs) to detect BSA on Ti alloy, before and after the chemical treatment of the surface, with also the possibility to gain information about conformational changes after protein adsorption.

Zeta (ζ) potential measurements have been largely employed in the study of nanoparticles [28] or powders [29] of various materials or to study and predict the stability of colloids [30,31]. Recently, they were also employed on bulk solid surfaces [32,33]. Regarding proteins, the shape of the titration curves is strictly dependent on the acidic and basic strength (pKa) of the exposed aminoacids functional groups and, their pKa may vary with denaturation or unfolding of proteins [34]. In this work, we explored the possibility of investigating the type of bonding of the proteins adsorbed onto the titanium substrates, alongside with the folding status.

The scope of this work is to demonstrate, for the first time, the applicability and potential of this set of complementary and innovative surface analyses for the characterization of a thin protein layer adsorbed on a surface with high biomedical interest, and to a mirror polished one as a control: the results can be used to further develop effective implants with multifunctional surfaces. The development of a suitable set of characterization techniques, able to investigate protein absorption on complex and real biomaterial surfaces, is of high interest for the biomaterials research community.

2. Materials and methods

2.1. Reagents

All the solutions and colloids were prepared by using highly pure reagents and water (Milli-Q). HCl (Carlo Erba, Milano, Italy) and HNO_3 (Carlo Erba, Milano, Italy) 3:1 v/v (aqua regia) were used to wash glassware. For the preparation of the treated titanium alloy samples, HF (Sigma-Aldrich, St. Louis, USA) and H_2O_2 (Panreac, Barcellona, Spain) were employed. Bovine serum albumin (BSA) (Sigma-Aldrich, St. Louis, USA) was purchased as powder. Phosphate buffered saline (PBS) solution was prepared by dissolving a tablet (Sigma-Aldrich, St. Louis, USA) in 200 ml of water. HCl and NaOH (Sigma-Aldrich, St. Louis, USA) were used to titrate the KCl (Sigma-Aldrich, St. Louis, USA) electrolyte solution for the zeta potential measurements.

For the synthesis of the spheroidal AgNPs, $AgNO_3$ (Panreac, Barcellona, Spain), $NaBH_4$ (Acros Organics) and sodium citrate tribasic dihydrate (Sigma-Aldrich, St. Louis, USA) were used. The synthesis method is reported in detail elsewhere [35] and can be found in the supplementary information.

2.2. Sample preparation

Ti6Al4V titanium alloy was purchased as cylindrical bar (ASTM B348, gr5, Titanium Consulting and Trading, Buccinasco, Italy) and cut into disks (1 cm diameter and 2 mm thick). The disks were polished using SiC papers, from 320 to 4000 grit, and subsequently washed in acetone (Supelco, Sigma-Aldrich, St. Louis, USA) and water (MilliQ), once for 5 min and twice for 10 min, respectively. After drying, they were stored in air until protein adsorption. Some disks underwent a chemical process to obtain a bioactive and hierarchically micro-nanostructured surface. It is a patented treatment which involves a first acid etching in hydrofluoric acid and a subsequent controlled oxidation in hydrogen peroxide [36,37]. The untreated and treated disks will be labelled hereafter Ti64 and Ti64CT, respectively.

Protein adsorption was carried on using a BSA (Sigma-Aldrich, St. Louis, USA) solution in PBS, prepared by dissolving tablets (Sigma-Aldrich, St. Louis, USA) in MilliQ water. BSA was dissolved in PBS in near-physiological concentration (20 mg/ml) [38] and pH 7.4 was reached by adding NaOH 0.05 M. Protein adsorption was obtained by placing the titanium samples in a 24-well plate and soaking them in 1 ml of protein solution at 37 °C for 2 h [32]. After that, the samples were gently rinsed 3 times with MilliQ water to remove loosely bound proteins, dried under laminar flow hood and stored at 4 °C prior being analysed. Samples after adsorption will be referred as Ti64 + BSA and Ti64CT + BSA. KPFM measurements required samples with half of the surface covered by proteins, in order to obtain a contrast in the potential image. They were prepared by spotting 50 μl of BSA solution on the surface, covering only half of it. Then they were incubated for 2 h at 37 °C in a humid chamber and rinsed and stored as before after drying.

2.3. X-ray photoelectron spectroscopy

Surface elemental composition was determined by X-ray photoelectron spectroscopy (XPS) (PHI 5000 VER-SAPROBE, Physical Electronics, Feldkirchen, Germany). Survey spectra were acquired on the whole set of samples prior and after protein adsorption, in order to assess BSA adsorption and to compare the total amount of adsorbed protein. XPS was performed also on the samples after zeta potential measurement in the acidic range. These samples will be referred as Ti64_z, Ti64 + BSA_z, Ti64CT_z, Ti64CT + BSA_z. The charging effect was compensated by setting the hydrocarbon C1s peak to 284.80 eV.

2.4. Kelvin force probe microscopy

Surface potential of samples was imaged by means of a Bruker Innova atomic force microscope (Billerica, USA) equipped with surface potential imaging tool. KPFM measurements were performed in lift mode, acquiring topographical image during the forward scan in tapping mode and the potential image during the backward scan in lift mode. Both the sample and the tip were grounded during the forward scan; to reduce artifacts due to sample charging, during the backward scan the sample was kept grounded and the tip was biased. In order to obtain images of the protein layer, Ti64 and Ti64CT samples were prepared so that BSA was adsorbed only onto a portion of the surface, as described in the sample preparation paragraph, and measured after drying. Topographical and surface potential images (100x80 μm) were obtained in the area of the border of the drop for visualizing the protein layer (scanning rate: 0.1 Hz; lift height: 300–500 nm; AC bias voltage: 3 V), while smaller scans (5x5 μm) (scanning rate: 1 Hz; lift height: 300–500 nm; AC bias voltage: 3 V) were performed on the portion of samples covered by albumin to evaluate the continuity of the layer. Samples were analyzed in air, in ambient conditions (humidity 35 ± 5%). Images were elaborated by using the Gwyddion software[39].

2.5. Surface Enhanced Raman scattering measurements

Raman measurements of BSA powder were collected with a dispersive Thermo Fisher Scientific DXR Raman microscope (Waltham, USA) equipped with an excitation laser source at 780 nm and a charge-coupled device (CCD) detector using 10 mW laser power, 10 X objective, rectangular aperture of 50 μm in a spectral range from 50 cm^{-1} to 3400 cm^{-1}. The acquisition time for each spectrum was 1 s for 25 exposures.

Raman equipment is weekly calibrated through a software-controlled calibration tool which corrects the frequency scale using multiple neon emission lines and, as a control, verifies the multiple polystyrene Raman peaks, while a white light source is used for the CCD calibration intensity. The grating resolution is 5 cm^{-1} (the grating density 900 lines/mm) and the uncertainty associated with the intensity is demonstrated to be lower than 5 % using a polystyrene standard. SERS measurements of liquid samples were performed using an accessory for liquid measurements with a quartz cuvette. The analysed liquid mixtures were composed of 30 nm AgNPs colloid and the concentrated BSA solution, in ratio 1:1.

SERS spectra on dried surfaces were collected after drop casting 10 μl of AgNPs suspension, air dried. Thermo Fisher Raman imaging DXR-Xi was used to collect maps of 500x500 μm (map resolution of 25 μm). 532 nm excitation laser was used, 1 mW laser power, 0.01 Hz collection frequency for 10 acquisitions on each map pixel. 10 X objective and rectangular 50 μm aperture was used. The spectra of the entire map were averaged to obtain one representative mean spectrum for the analyzed area.

2.6. Attenuated total Reflectance Mid-Infrared spectroscopy

IR spectroscopy is a well-established technique for the study of protein adsorption on titanium surfaces and their conformational changes after interaction with the surface [7]. In this work, ATR-FTIR was used in order to confirm the results and information obtained by the other techniques. ATR-MIR measurements were performed with a FT-IR spectrometer (Nicolet iN10 Infrared Microscope, Thermo Fischer Scientific, Waltham USA). Se/Ge ATR tip was used to investigate the samples, the cooled MCT detector was selected to collect the spectra in the range 1000–4000 cm^{-1} with a resolution of 4 cm^{-1} with 64 scansions for each spectrum. The spectral background was acquired with the ATR tip in air before every measurement.

2.7. Zeta potential of reference solution and solid surfaces

Zeta potential titration curves of BSA solution were obtained using dynamic light scattering (DLS) instrument (Litesizer 500, Anton Paar, Graz, Austria). Measuring solutions were prepared by dissolving BSA in PBS at an initial concentration of 35 mg/ml, followed by aliquoting with KCl 0.001 M to a final concentration of 5 mg/ml. The pH was adjusted by HCl and NaOH to the following values: 2.5, 3, 3.5, 4, 5, 6, 7, 8, 9. Untreated and treated titanium disks were analyzed by means of an electrokinetic analyzer (SurPASS, Anton Paar, Graz, Austria) equipped with an automatic titration unit. The samples were mounted using an adjustable gap cell

and the measurement was performed using KCl 0.001 M as electrolyte. NaOH and HCl 0.05 M were used for titration in the basic and acid range, respectively and fifteen points have been measured for each range. Titration curves were obtained before and after soaking in BSA solution. A new couple of specimens was used for each range to avoid artifacts due to reactions that may occur during the measurement.

3. Results and discussion

The results of a detailed investigation of adsorbed BSA on bare (Ti64) and chemically treated (Ti64CT) titanium surfaces are here reported and compared, including investigation of the presence (XPS survey), distribution (KPFM), eventual unfolding of the protein (ATR-IR and Raman-SERS) and type of the chemical interaction with the substrate (zeta potential titration curves followed by XPS surface analysis). Ti64CT is an interesting example of a surface for implants to be integrated in hard or soft tissues [37] which cannot be easily investigated in detail after protein adsorption with the conventional protocols of characterization because of roughness and surface chemistry.

3.1. XPS compositional analysis

The actual presence of adsorbed proteins on the surfaces can be verified by investigating the surface chemical composition, in particular the C and N content. N is commonly used as an indicator of proteins adsorbed onto titanium surfaces, being absent on bare titanium and in adventitious contaminants. The elemental composition of the samples is reported in Table 1.

The reference samples (Ti64, Ti64CT) show the typical elements of titanium oxide: Ti and O. As expected, Ti64CT has a higher oxygen concentration than Ti64 due to higher surface hydroxylation [37], which is also confirmed when the composition is evaluated without considering the carbon contaminations (Table 1S, supporting information. Differences in the Ti chemical state were also observed, with an slight increase of Ti(IV) with respect to Ti(III) and the disappearance of Ti(0) (Fig. 1S and Table 2S, supporting information). Those results agree with the fact that the newly formed oxide layer, thicker than on untreated Ti, has a $H_2Ti_3O_7$ composition, as previously published by the authors [40], which has an higher oxygen content and more Ti^{4+} than the native oxide tri-layer TiO_2-Ti_2O_3-TiO suggested for titanium surfaces [41]. Al and V are expected to be undetected due to their absence within the oxide layer and limited penetration depth of XPS: XPS analysis is mainly limited to the TiO_2 surface layer even on untreated Ti64. The XPS depth of analysis is proportional to the inelastic mean free path (IMPF) of electrons generated by the samples, which is due, among other things, by the kinetic energy (KE) of such electrons and by the composition of the material itself [42]. Due to the complex chemistry of the treated oxide layer and the uncertain thickness of the native oxide on Ti64, the IMPF can not be exactly determined. Still, an estimation can be done considering the surfaces as only composed by TiO_2: in this case, electrons with a KE in the range of 600 to 1200 eV have an IMPF lower than 2 nm [43]. The carbon content on Ti64 and Ti64CT is due to hydrocarbon adventitious contaminations from atmosphere, always present since titanium is readily contaminated when exposed to air [44].

After protein adsorption, the C and N content increase on both surfaces (Ti64 + BSA and Ti64CT + BSA), as expected. N was not found on the pristine samples, while it is around 10% after protein adsorption. At the same time, the atomic percentage of both Ti and O decreases after protein adsorption, suggesting that BSA forms a continuous layer on both samples able to almost mask the substrate to XPS analysis. This is confirmed by the fact that a N atomic concentration of about 9% is reported as reference for saturation of an adsorbed protein [45]. A slightly higher N content on Ti64CT compared to Ti64 is a first evidence that the treated surface can bind a ticker layer of the protein: this was confirmed by the authors with other techniques, such as bicinchoninic acid protein assay (Fig. 2S, supporting information). The larger amount of BSA for the chemically-treated titanium sample can be the result of two factors. The treated surface has higher surface area than the polished sample and nanopores can accommodate the proteins with a larger number of sites of interaction between the protein and surface. This effect can be fostered by a higher density of OH groups, as it will be further discussed in section 3.4 and 3.5, even if it was not expected considering the general rule that proteins adsorb more and more strongly on hydrophobic surfaces and that the main driving force for adsorption is the hydrophobic interaction [7].

3.2. Kelvin probe force microscopy

KPFM was employed as an imaging technique to map the protein layer adsorbed on the surface of the samples and to investigate its homogeneity.

The topographical and surface potential images obtained at the border of a protein spot for both Ti64 and Ti64CT are shown in Fig. 1. In the topographical images, the surfaces appear homogeneous: the Ti64 surface shows the signs of the gritting papers, while the Ti64CT exhibits a globular microroughness that it is created after the chemical treatment, due to uneven etching of the α and β phases of the alloy and the formation of a sponge-like oxide layer, as was also observed by electron microscopy (Fig. 3S, supporting information) [37]. The average roughness value, S_a, increases from 0.048 ± 0.011 to 0.250 ± 0.027 μm (Table 3S). The protein layer is indistinguishable in the topographical image, indicating that its thickness is in the range of few nanometers, which can correspond to about a monolayer or very few layers of albumin molecules. This is a first relevant information, because surface-engineered biomaterials for osseointegration must exhibit their peculiar topography and roughness to the cells, after protein adsorption, to be effective and it was confirmed by observations at larger magnification (see below).

On the other hand, the surface potential images clearly show a border, which separates two areas with different potential, and corresponds to the border of the protein spot: the areas where albumin was allowed to adsorb are at a lower surface potential with respect to the titanium surfaces. This fact agrees with literature, adsorbed biological molecules, such as protein and DNA, have a lower potential with respect to the adsorbent surface [46,47], and this was also reported for albumin on Ti6Al4V surfaces [21].

Table 1
Surface chemical composition of the samples before and after albumin adsorption (atomic %). Undetected elements are marked with a dash.

	C	O	N	Ti	Al	V	Other elements
Ti64	46.3	38.0	–	11.6	3.2	–	0.8
Ti64CT	28.4	57.2	–	14.4	–	–	–
Ti64 + BSA	58.3	25.5	9.7	4.2	–	–	2.3
Ti64CT + BSA	55.0	29.6	11.4	4.0	–	–	–

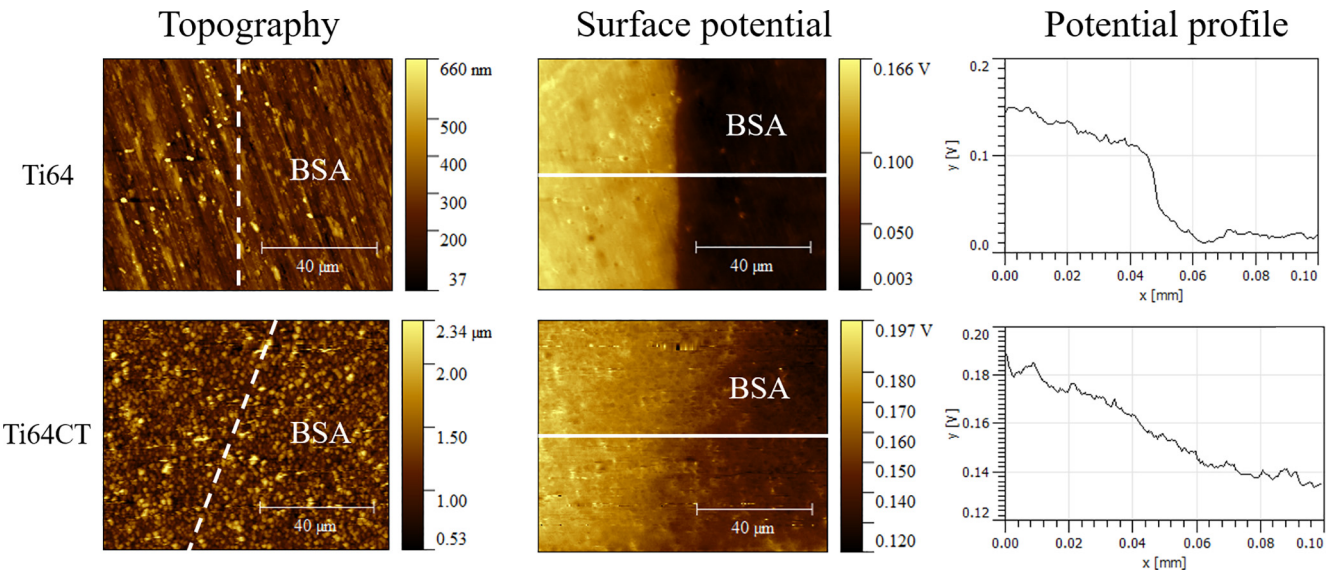

Fig. 1. Atomic force microscopy of Ti64 (top) and Ti64CT (bottom) surfaces half covered with BSA. Scan size is 100x80 µm. Left: AFM topographical images, the white dotted lines represent the border of the BSA layer; center: KPFM surface potential images of the same area; right: potential profiles along the white line on the potential images.

This observation suggests that a continuous protein layer is formed on both surfaces, where they were exposed to the protein solution (right side of the surface potential images). This is a further interesting information considering that protein agglomeration on the micro scale can occur in some cases after surface adsorption [48].

The Ti64 specimen has a sharp border, related to a highly confined BSA solution drop, due to the quite low wettability of Ti64 (see supporting information). The protein layer is very homogeneous and continuous on the entire surface, showing a surface potential about 115 mV higher with respect to the clean substrate. On the other hand, the Ti64CT sample shows a smoother border between the areas with or without BSA. The higher roughness and the higher wettability, as shown by contact angle measurement (described in the supporting information), with respect to the Ti64 surface lead to a more spread drop of the protein solution. In this case, the difference in surface potential between the treated titanium surface uncovered by albumin and the portion with BSA is about 40–50 mV. This reduced voltage difference, with respect to Ti64, may be caused by very different work functions of the different titanium oxide phases and, as consequence, different surface potential [49]; it is known that the chemical treatment changes the titanium oxide phase with respect to the native oxide layer on Ti64. The surface potential difference may be also influenced by the presence of sub-microroughness and nanopores, which can limit the electrostatic interactions between the tip and the proteins. It is also possible that this slightly affects the resolution of the KPFM. On both surfaces, the absolute value of the electric potential of the adsorbed albumin layer might be influenced by the adsorption of some ions from the PBS solution, but it does not affect the imaging of the protein distribution on the surface through KPFM.

Small scans, 5*5 µm, were performed with KPFM in order to assess the continuity of the BSA layer at higher magnification, on both substrates, in the area where albumin adsorption occurred (Fig. 2). The topography within the area with adsorbed BSA is similar to the one without protein (here not shown), which is reasonable accounting for the presence of a thin adsorbed layer. The observed surface potential variation within this area is about 15 mV, for each substrate, which is much lower that what observed between the pristine and adsorbed areas in Fig. 1, confirming that the protein layer is continuous. Considering the crucial role of roughness and surface morphology in determining cell adhesion and differentiation, it is interesting to verify that the surface topography of Ti64CT is not hidden by protein adsorption and that protein aggregates are not visible even at this larger enlargement. In the potential image of Ti64CT + BSA, a well-defined area at higher potential was observed, corresponding to a protruding element in the topographical image (white circle in Fig. 2). As possible to see also from SEM micrographs (Fig. 2S, supporting information), those features corresponds to β-phase grains, which have been reported to have an higher surface potential than α-phase [21]: the potential image of the BSA layer can be affected by the potential of the substrate, due to its very low thickness.

It can be concluded that KPFM allows the investigation of protein distribution on a rough surface at a micrometrical scale.

3.3. Raman measurements

The Raman spectra of the BSA powder were at first collected as reference (see supplementary information, Fig. 3S). Native α-helix structure was compared with unordered BSA obtained by thermal denaturation, heating albumin at 100 °C for 1 h. As previously reported in literature, we confirmed that the Raman peak of Amide I at 1650 cm^{-1} is shifted at slightly higher frequency (1660–1670 cm^{-1}) after denaturation of the protein [50].

Since poor sensitivity of Raman does not allow to detect the thin layer of BSA adsorbed on the Ti alloy surface, SERS strategy to enhance BSA signals was implemented by using an Ag colloid (spheroidal AgNPs with 30 nm of diameter) as a SERS substrate directly deposited on the surface to be probed. Several studies already proposed metallic NPs as useful substrates for biomolecules detection [51], where a chemical interaction between the colloids and the analyte occurred [52]. The chemical binding of the analyte to the NPs can lead to the clustering of NPs providing SERS hot spots responsible for the Raman enhancement [53]. The interactions between albumin and AgNPs was investigated in order to evaluate if they provoke any denaturation (supporting information), and it was found that the Amide I band of BSA was not shifted by the nanoparticles, neither in solution nor when drop-casted onto protein-adsorbed surfaces (Figure 6S and 7S, supporting information).

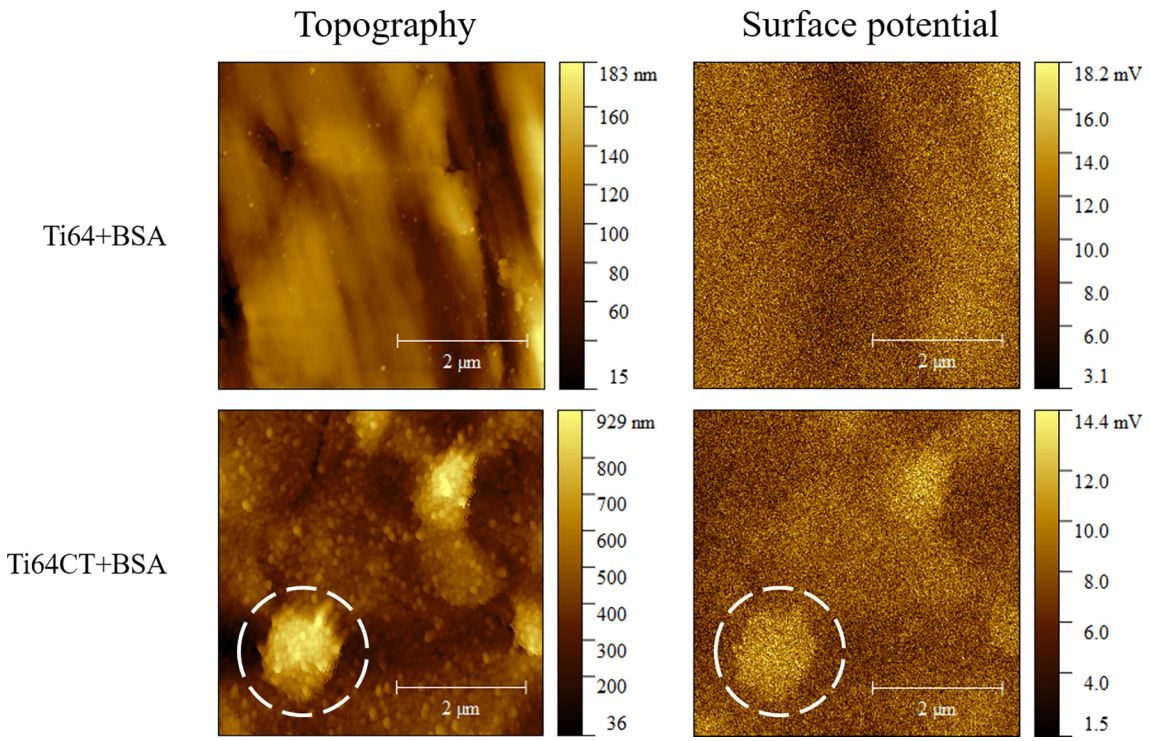

Fig. 2. Topography (left column) and surface potential images (right column) of Ti64 + BSA (top row) and Ti64CT + BSA (bottom row) surfaces. Scan size is 5x5 µm.

After the preliminary investigations, AgNPs were drop casted on the Ti64 polished and chemically-treated alloy (CT) samples, with or without (as control (CTRL) test) adsorbed BSA, and the SERS spectra were collected (Fig. 3). On both substrates, the enhancement effect provoked by the metal nanoparticles allowed to detect the characteristic Amide I peak on the adsorbed surfaces.

On the polished alloy, a peak at 1658 cm^{-1}, corresponding to α-helix conformation, is present after adsorption (Ti64 + BSA) and a shoulder at 1670 cm^{-1} is also visible, evidencing a partial denaturation of the protein chain [54]. Even if some interfering signals are present on the Ti64 surface (Fig. 3, spectrum b), the albumin adsorbed onto the surface is clearly detectable with SERS, and a partial conformation change of the adsorbed protein is suggested.

Analogously, it was possible to determine the position of the Amide I peak of BSA adsorbed on the chemically treated alloy, having an idea of its secondary structure after adsorption. The amide I peak is shifted at 1670 cm^{-1} attesting the loss of native α-helix conformation and evidencing denaturation of the adsorbed BSA

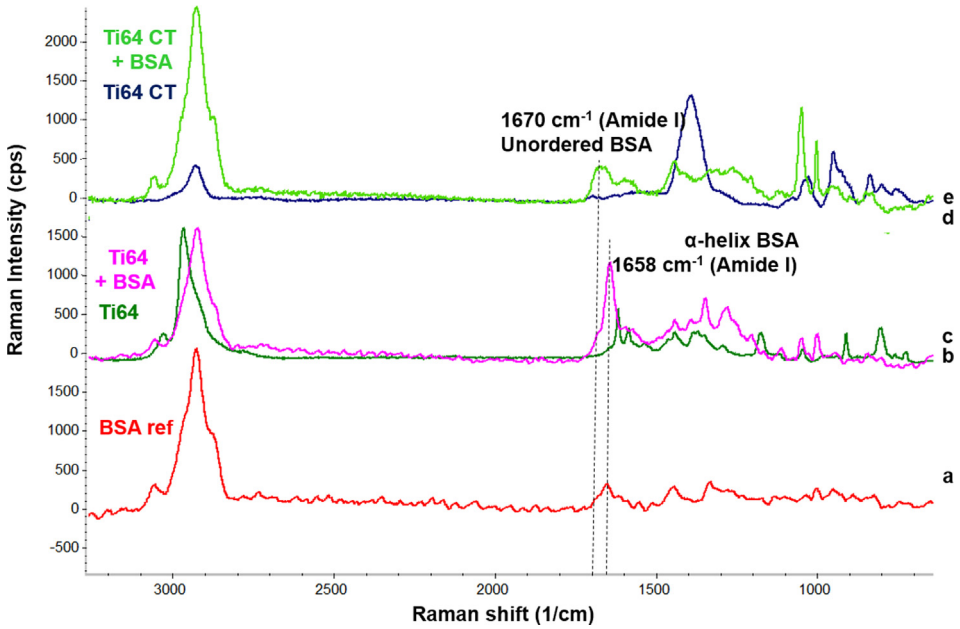

Fig. 3. SERS spectra of a) BSA powder as reference, b) Ti64 - negative CTRL of Ti polished alloy, c) Ti64 + BSA - BSA deposited on Ti polished alloy, d) Ti64CT - negative CTRL of chemically treated Ti alloy, e) Ti64CT + BSA: BSA deposited on chemically treated Ti alloy.

on Ti64CT. In this case, unlikely to what happens with Ti64, no interfering signals are present in the SERS spectra of the control sample.

The greater loss of ordered structures of albumin when adsorbed on Ti64CT than on Ti64 is reasonable considering the possible interactions between the protein and the surface, resulting in higher affinity of BSA with the Ti surface after the chemical treatment. Acidic hydroxyl groups are formed with high surface density on CT samples, and it is well acknowledged that an increase in hydroxylation degree of titanium surfaces leads to higher and stronger albumin adsorption [55]. As discussed by Oliva et al. [56], the main interactions between titanium and albumin, adsorbed at pH above 7, are electrostatic interactions and hydrogen bonding. The former can occur between mono-coordinated OH (basic) groups on titanium and protein ammonium or carboxylate groups and between di-coordinated surface (acidic) OH and $-NH_3^+$ groups of albumin. The latter occur between mono-coordinated OH and positive ammonium groups. The reactions are described below [56]:

Basic Ti-OH-ammonium group electrostatic interaction:

$>Ti\text{-}OH + R\text{-}NH_3^+ \rightarrow >Ti\text{-}OH_2^+:NH^2\text{-}R$.

Basic Ti-OH-carboxylate group electrostatic interaction:

$>Ti\text{-}OH + R\text{-}COO^- + H_2O \rightarrow >Ti\text{-}OH_2^+{}^-OOC\text{-}R + OH^-$.

Acidic Ti-OH-ammonium group electrostatic interaction:

$>Ti_2 = O^- + R\text{-}NH_3^+ \rightarrow >Ti_2 = O^+NH_3\text{-}R$.

Basic Ti-OH-ammonium group hydrogen bonding interaction:

$>Ti\text{-}OH + R\text{-}NH_3^+ \rightarrow >Ti\text{-}OH\text{---}:NH^2\text{-}R$.

On the Ti64CT surface there is a predominance of acidic OH groups, but some monocoordinated hydroxyls are present [57]. As consequence, the main protein-surface interactions can be acidic OH-ammonium group electrostatic interactions, but also the other kind of interactions, such as hydrogen bonding, can play a role in BSA adsorption.

These facts can explain both the higher amount of protein adsorbed by Ti64CT substrate, as previously introduced in section 4.1, and the more denatured conformation of BSA on the same surface with respect to the untreated Ti alloy. It will be of interest to verify with *in vitro* and *in vivo* tests the impact of this type of protein denaturation on the biological response to a surface for osseointegration.

3.4. ATR-IR measurements

Attenuated Total Reflectance-MIR is an acquisition mode particularly suitable for the analysis of thin films, such as a protein layer [58]. This technique is here used with two aims: confirmation of the presence of the adsorbed protein obtained with the innovative SERS approach, and of eventual changes of the molecular structure after the adsorption process. Quantification of the adsorbed albumin is reported on titania nanotubes through the analysis of the intensity of the Amide I band [59]; deconvolution of the same band can be employed to determine the secondary structure of the adsorbed protein [60]. It was necessary to use micro-FTIR equipped with ATR tip since the standard ATR has not enough sensitivity to detect the thin layer of adsorbed proteins.

The ATR-IR spectra of the blank sample of the polished alloy (Ti64) (Fig. 4, spectrum b) has no absorption peaks, as expected. This allows to precisely determine that the amide I peak of BSA adsorbed on the metal surface is little blue-shifted with respect to the α-helix Amide I characteristic mode (Fig. 4, spectrum c). This confirms that adsorption of the protein on Ti64 causes a partial conformational change in the polypeptide chains from α-helix towards β-turns [61].

Conversely, the chemically-treated alloy, both without and with BSA, (Fig. 4, spectra d,e) presents a spectrum dominated by an intense and broad band at 3400 cm^{-1} due to the hydroxyl groups on the surface of the CT sample. This is certainly due to the oxidation process that occurs on the sample surface during the chemical treatment. Considering that titanium surfaces with high hydroxylation degree have several benefits in terms of wettability and biological response (bone integration and inflammatory response), this is not unusual on clinically-used titanium surfaces. In the amide region (1650 and 1530 cm^{-1}), unfortunately, two intense peaks, at about 1625 and 1427 cm^{-1} respectively, are present even on the control sample (Ti64CT - Fig. 4, spectrum d) and these signals interfere with the BSA signal on Ti64CT + BSA. Those peaks can be attributed to the hydroxyl groups on the surface [62]. Although the interfering signals of the substrate, the presence of the protein on Ti64CT + BSA is still detectable from the ATR-IR spectrum (Fig. 4, spectrum e). Concerning investigation of the molecular structure, the peak at 1660 cm^{-1} is slightly more intense and red-shifted in the adsorbed sample, due to the contribution of Amide I. However, the overlap of the ATR-IR bands due to the substrate prevents any precise conformational determination of the protein adsorbed on the chemically-treated Ti alloy, since the peak position is influenced by the overlapping ATR-IR band of the substrate. These analyses evidence that this technique is not perfectly suitable to compare the molecular structure of adsorbed proteins on surfaces for osseointegration, such as chemically treated titanium with high density of surface OH groups.

3.5. Zeta potential titration curve of native BSA and solid surfaces

Zeta potential titration curves were obtained in the pH range 2.5–9.5 for native albumin, in solution, and on the substrates before and after protein adsorption (Fig. 5).

At first, the chemical treatment of the titanium alloy causes a shift of the IEP from 4.9 (Ti64), which is in the range reported in literature [63], to a value below 3 (Ti64CT), not reached in the measurement range, but obtainable by interpolation. As discussed deeply in a previous work [32], the shift in the IEP and the formation of a plateau in the basic range (absent in the case of Ti64), with onset at pH = 5.1, are due to the increase of surface hydroxylation after the chemical treatment and to the acidic behaviour of the OH groups. As result, Ti64CT has a surface with higher density of OH, with respect to Ti64, and they are fully deprotonated at pH 7.4 when protein adsorption occurs.

By analysing the titration curves reported in Fig. 5-b, it is possible to notice that adsorption of albumin drastically changes the surface potential of Ti64CT, in agreement with a complete coverage of the surface by the protein as confirmed by the N values obtained by XPS and the KPFM images. On the other hand, the zeta potential titration curve of Ti64 does not change significantly after adsorption of BSA (Fig. 5-a), despite the protein presence on Ti64 + BSA has been detected and confirmed by all the other techniques. As it will be discussed in a deeper manner below, this may be due to a partial detachment of the protein during the zeta potential measurement and consequent exposure of the bare titanium alloy. Thereby, the resulting ζ potential is a combination from the surface and the residual adsorbed protein. The IEP of Ti64CT + BSA is at pH 4.5 as the one of albumin (here experimentally detected in solution and in agreement with literature [64]), here confirming the complete surface coverage by the protein. The zeta potential titration curve provides also different information on the chemistry of the sample's suface. In fact, the shape of the zeta potential titration curve of a protein is related to the dissociation of the NH_3^+ or protonation of the COO^- groups. The pKa of the amino groups, in particular of Lysine and Arginine, is very high (>9) [65], thus these groups are protonated on all the tested pH range. On the other hand, the pKa of the acidic residues, aspartic and glutamic acid, is around 4 [65]. Thus, they change their protonation states during the titration measurement, within a few pH units around the pKa.

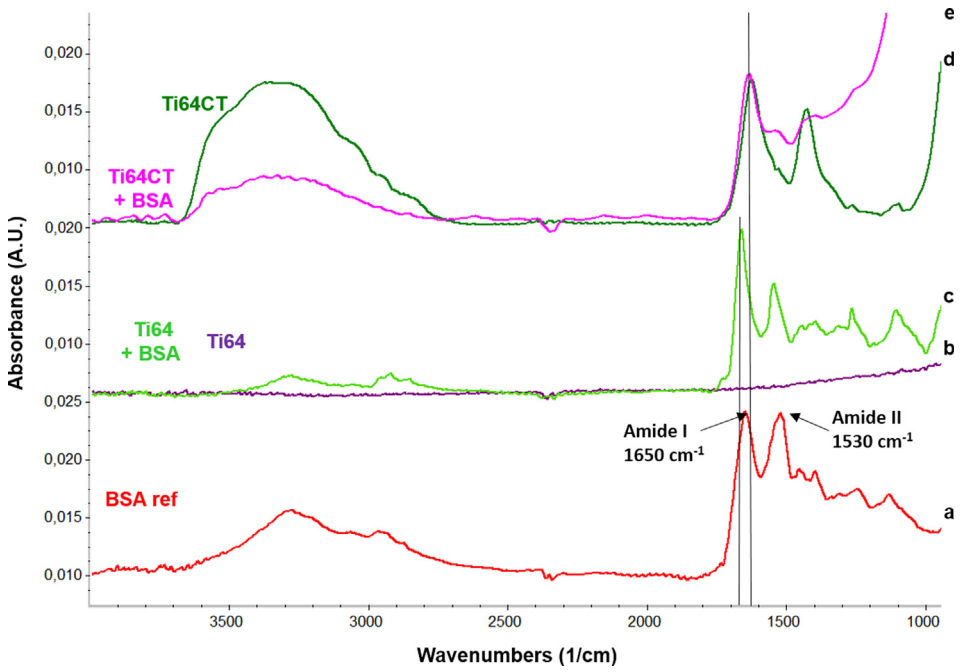

Fig. 4. ATR spectra of a) BSA powder as reference, b) Ti64: negative CTRL of Ti polished alloy, c) Ti64 + BSA: BSA deposited on Ti polished alloy, d) Ti64CT: negative CTRL of chemically treated Ti alloy, e) Ti64CT + BSA: BSA deposited on chemically treated Ti alloy.

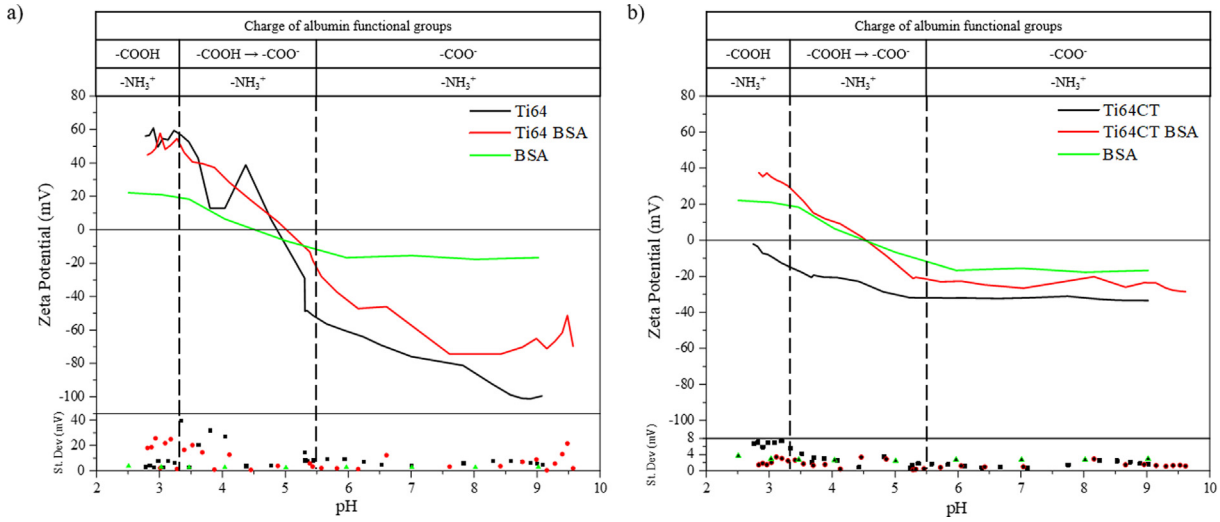

Fig. 5. Zeta potential titration curves for untreated Ti64 (a), prior (black line) and after (red line) protein adsorption, and for Ti64CT (b), prior (black line) and after (red line) protein adsorption. The titration curve of native albumin in solution is also reported (green line). Standard deviations for each measured point are represented at the bottom of the graphs. The charge of the functional groups of the amino acids of BSA is reported on the top of the graphs for the different pH ranges.

In the acidic plateau, both the functional groups are protonated and the protein is positively charged due to NH_3^+ groups. Lowering the pH value of the solution, the acidic plateau ends when the COOH groups begin to dissociate and, as consequence, the overall net charge of the protein decreases. The IEP is reached when the number of dissociated carboxyl groups are equal to the number of the protonate amino ones. At the onset of the basic plateau, the carboxyl groups are fully in the COO^- form [66]. The net charge of the protein is negative due to the fact that the acidic amino acid residues are almost twofold than the basic amino acid ones in the BSA peptide chain [67]. The shape of the titration curve of albumin is dictated in particular by the pKa of the carboxyl group of the aspartic and glutamic residues.

The curve of Ti64CT + BSA is different from the one of BSA in solution, in particular regarding the onset of the plateaux. BSA in solution showed the onset of the acidic and basic plateaux respectively at about pH 5.5 and 3.3. On the other hand, the basic plateau essentially disappeared and the onset of the acidic one is down-shifted to pH about 5.3 on Ti64CT + BSA. These shifts may be ascribed to changes in the acidic strength of the carboxyl groups, related to changes in their chemical environment. Since the pKa of the $-COO^-$ groups may be lowered upon protein unfolding [34], the zeta potential measurement can be explained considering that BSA adsorbs onto Ti64CT with a denatured conformation. This is in agreement with the findings obtained through SERS analysis.

Due to the partial removal of albumin from the polished surface during the zeta potential titration measurement, it is not possible

to comment the curve obtained on Ti64 + BSA samples since it is impossible to separate the contribution to the titration curve coming from the metal substrate from the one of adsorbed albumin. A detachment of the adsorbed albumin is suggested by the zeta potential titration curve of Ti64 + BSA in the range between pH 4 and 5, where there is an increase of the standard deviations, which accounts for an ongoing surface modification [40]. In order to confirm this, XPS was performed on the samples that underwent the acidic range of the titration curves and the content of carbon and nitrogen was evaluated. The C atomic content is similar on Ti64_z, Ti64 + BSA_z (the samples analysed after the zeta potential measurement – Table 2) and on pristine Ti64 (Table 1); on Ti64 + BSA_z, the N level is about half what it was before the electrokinetic analysis. These data confirm that adsorbed albumin is significantly removed from the untreated titanium alloy surface during the zeta potential measurement. Therefore, the titration curve of Ti64 + BSA reflects this phenomenon and evidences an instability of the chemical bond between the adsorbed protein and the surface when the pH goes down to pH 4.5, as in case of inflammatory conditions: the instability of the protein layer can be attributed to weak protein-surface interactions, caused by a low density of hydroxyl surface groups on the untreated titanium that limits the binding sites for albumin, allowing the detachment by changing pH of the solution in contact with the adsorbed layer.

On the other hand, no evident increment of standard deviation was observed in the case of the zeta potential titration curve of Ti64CT + BSA (standard deviation is below 5 mV along all the measurement range): this surface is chemically stable in the explored range of pH. In agreement with this result, the C and N values obtained through XPS on Ti64CT + BSA_z are much higher than the Ti64CT_z ones and they are close to the data obtained for Ti64CT + BSA, well above the threshold value for surface saturation by the adsorbed proteins [45]. This set of data suggests that BSA is more strongly bound on Ti64CT than on Ti64, thus it is not removed from the surface during the zeta potential measurement even at low pH such as in inflammatory condition. The hydroxylation degree of the surfaces and the chemical behaviour of their OH groups seem to play a major role in defining the stability and strength of protein-surface bonds.

According to these data, the obtained zeta potential titration curves are significant of the type of bond of the adsorbed protein with a surface as well as of eventual unfolding. Albumin, which is an anti-inflammatory protein, plays a major role in long term osseointegration: a large and strong adsorption of this protein in both inflammatory and physiological conditions can be beneficial in avoiding chronic inflammation and the consequent implant failure (as happens on very rough surfaces) [1]. Further studies will be performed to evaluate the effect of the different adsorption of BSA in terms of modulation of the inflammatory response by the different biosurfaces. Further investigations shall be also conducted on proteins relevant in the osseointegration process, such as fibronectin, which can increase the adhesion of osteoblasts. An enhanced and selective adsorption of both these proteins on the chemically-treated surface would confirm the potential of this surface as bone-implantable biomaterial.

Table 2
C and N content (atomic %) of Ti64 and Ti64CT before and after protein adsorption after zeta potential measurement in the acidic range.

	C [% at]	N [% at]
Ti64_z	42.2	2.3
Ti64 + BSA_z	40.8	5.1
Ti64CT_z	36.5	0.0
Ti64CT + BSA_z	55.7	11.9

4. Conclusions

In this work, we suggest a novel approach which can be used to characterize protein adsorption, in terms of surface coverage and distribution, protein conformation, type, and strength of the surface-protein interaction, addressing a well known issue among researchers [68]; traditional techniques such as ATR-IR and XPS can be used to support and confirm the results. Furthermore, we prove that the selected set of techniques can be applied to surfaces relevant for medical implants, with surface topography and chemistry precisely developed for osseointegration, and not only on model flat surfaces [20,26].

The adsorbed protein (BSA) layer was visualized by means of KPFM, proving that albumin forms a continuous layer on both pristine (Ti64) and chemically treated (Ti64CT) Ti surfaces when adsorbed from near physiological concentration. The results agree with XPS and zeta potential titration data. Protein quantification by BCA shows that the chemical treatment is effective for enhancing the adsorption of proteins on the titanium surface. It was observed that proteins form a thin layer on all the surfaces, not being able to mask even the sub-microtopography of the microrough surface (Ti64CT).

The conformation, chemical stability, and type of bonding with the surface of the adsorbed protein were investigated by a novel and simple approach based on SERS and zeta potential analysis; XPS is useful for confirmation of the data. Protein adsorption on titanium substrates is strongly driven by the degree of hydroxylation of the surface. A higher number of OH groups, as in the case of Ti64CT, increases the interactions with BSA, through electrostatic and hydrogen bonds, leading to a larger quantity of adsorbed protein, more strongly bonded (even at inflammatory pH) and, as consequence, more denatured than in the case of the untreated Ti64 surface. The effect of various degrees of surface hydroxylation on the adsorption of proteins is a very interesting outcome of this work and it request further investigations, which are ongoing. In the light of these results, it seems necessary to reconsider the general rule that proteins adsorb more and in a stronger way on hydrophobic surfaces and that the main driving force for adsorption is the hydrophobic interaction [9], on titanium-based biomaterials at least.

Declaration of competing interest.

The authors declare that they have no known competing financial interests or personal relationships that could have appeared to influence the work reported in this paper.

Data and materials availability

All data needed to evaluate the conclusions in the paper are present in the paper and/or the Supporting Information.

CRediT authorship contribution statement

Jacopo Barberi: Conceptualization, Investigation, Writing – original draft, Writing – review & editing. **Sara Ferraris:** Writing – review & editing. **Andrea Mario Giovannozzi:** Methodology, Writing – review & editing. **Luisa Mandrile:** Investigation, Methodology, Writing – original draft, Writing – review & editing. **Erik Piatti:** Investigation, Methodology, Writing – review & editing. **Andrea Mario Rossi:** Funding acquisition, Supervision, Writing – review & editing. **Silvia Spriano:** Conceptualization, Funding acquisition, Methodology, Supervision, Writing – review & editing.

Declaration of Competing Interest

The authors declare that they have no known competing financial interests or personal relationships that could have appeared to influence the work reported in this paper.

Acknowledgments

The authors want to acknowledge Dr. Matteo Berruto and Dr. Iris Cagnasso for AgNPs preparation and Dr. Lucia Napione for performing the BCA assay. This research was in part performed in the IMPreSA Infrastructure laboratories, funded by Regione Piemonte and INRIM. This research did not receive any specific grant from funding agencies in the public, commercial, or not-for-profit sectors.

Appendix A. Supplementary data

Supplementary data to this article can be found online at https://doi.org/10.1016/j.matdes.2022.110712.

References

[1] S. Spriano, S. Yamaguchi, F. Baino, S. Ferraris, A critical review of multifunctional titanium surfaces: New frontiers for improving osseointegration and host response, avoiding bacteria contamination, Acta Biomater. 79 (2018) 1–22, https://doi.org/10.1016/j.actbio.2018.08.013.
[2] S.R. Kandavalli, Q. Wang, M. Ebrahimi, C. Gode, F. Djavanroodi, S. Attarilar, S. Liu, A Brief Review on the Evolution of Metallic Dental Implants: History, Design, and Application, Front. Mater. 8 (2021), https://doi.org/10.3389/fmats.2021.646383.
[3] X. Lu, Z. Wu, K. Xu, X. Wang, S. Wang, H. Qiu, X. Li, J. Chen, Multifunctional Coatings of Titanium Implants Toward Promoting Osseointegration and Preventing Infection: Recent Developments, Front. Bioeng, Biotechnol. 9 (2021) 1–19, https://doi.org/10.3389/fbioe.2021.783816.
[4] J. Xu, J. Zhang, Y. Shi, J. Tang, D. Huang, M. Yan, M.S. Dargusch, Surface Modification of Biomedical Ti and Ti Alloys: A Review on Current Advances, Materials (Basel). 15 (2022) 1749, https://doi.org/10.3390/ma15051749.
[5] G. Louarn, L. Salou, A. Hoornaert, P. Layrolle, Nanostructured surface coatings for titanium alloy implants, J. Mater. Res. 34 (2019) 1892–1899, https://doi.org/10.1557/jmr.2019.39.
[6] T. Hanawa, Titanium-tissue interface reaction and its control with surface treatment, Front. Bioeng. Biotechnol. 7 (2019), https://doi.org/10.3389/fbioe.2019.00170.
[7] J. Barberi, S. Spriano, Titanium and protein adsorption: An overview of mechanisms and effects of surface features, Materials (Basel). 14 (2021), https://doi.org/10.3390/ma14071590.
[8] E. Mariani, G. Lisignoli, R.M. Borzì, L. Pulsatelli, Biomaterials: Foreign bodies or tuners for the immune response?, Int J. Mol. Sci. 20 (2019), https://doi.org/10.3390/ijms20030636.
[9] M. Rabe, D. Verdes, S. Seeger, Understanding protein adsorption phenomena at solid surfaces, Adv. Colloid Interface Sci. 162 (2011) 87–106, https://doi.org/10.1016/j.cis.2010.12.007.
[10] C. Guder, S. Gravius, C. Burger, D.C. Wirtz, F.A. Schildberg, Osteoimmunology: A Current Update of the Interplay Between Bone and the Immune System, Front. Immunol. 11 (2020) 1–19, https://doi.org/10.3389/fimmu.2020.00058.
[11] R. Trindade, T. Albrektsson, P. Tengvall, A. Wennerberg, Foreign Body Reaction to Biomaterials: On Mechanisms for Buildup and Breakdown of Osseointegration, Clin. Implant Dent. Relat. Res. 18 (2016) 192–203, https://doi.org/10.1111/cid.12274.
[12] R.M. Visalakshan, M.N. Macgregor, S. Sasidharan, A. Ghazaryan, A.M. Mierczynska-Vasilev, S. Morsbach, V. Mailänder, K. Landfester, J.D. Hayball, K. Vasilev, Biomaterial Surface Hydrophobicity-Mediated Serum Protein Adsorption and Immune Responses, ACS Appl. Mater. Interfaces. 11 (2019) 27615–27623, https://doi.org/10.1021/acsami.9b09900.
[13] H. Felgueiras, V. Migonney, S. Sommerfeld, N.. Murthy, J. Kohn, Competitive Adsorption of Albumin, Fibronectin and Collagen Type I on Different Biomaterial Surfaces: A QCM-D Study, in: L.M. Roa Romero (Ed.), IFMBE Proc., Springer International Publishing, Cham, 2014: pp. 563–566. 10.1007/978-3-319-00846-2.
[14] M. Pegueroles, C. Tonda-Turo, J.A. Planell, F.-J. Gil, C. Aparicio, Adsorption of Fibronectin, Fibrinogen, and Albumin on TiO 2: Time-Resolved Kinetics, Structural Changes, and Competition Study, Biointerphases. 7 (2012) 48, https://doi.org/10.1007/s13758-012-0048-4.
[15] W. Melitz, J. Shen, A.C. Kummel, S. Lee, Kelvin probe force microscopy and its application, Surf. Sci. Rep. 66 (2011) 1–27, https://doi.org/10.1016/j.surfrep.2010.10.001.
[16] S. Metwally, S. Ferraris, S. Spriano, Z.J. Krysiak, Ł. Kaniuk, M.M. Marzec, S.K. Kim, P.K. Szewczyk, A. Gruszczyński, M. Wytrwal-Sarna, J.E. Karbowniczek, A. Bernasik, S. Kar-Narayan, U. Stachewicz, Surface potential and roughness controlled cell adhesion and collagen formation in electrospun PCL fibers for bone regeneration, Mater. Des. 194 (2020), https://doi.org/10.1016/j.matdes.2020.108915 108915.
[17] Ł. Kaniuk, S. Ferraris, S. Spriano, T. Luxbacher, Z. Krysiak, K. Berniak, A. Zaszczynska, M.M. Marzec, A. Bernasik, P. Sajkiewicz, U. Stachewicz, Time-dependent effects on physicochemical and surface properties of PHBV fibers and films in relation to their interactions with fibroblasts, Appl. Surf. Sci. 545 (2021), https://doi.org/10.1016/j.apsusc.2021.148983 148983.
[18] A.K. Sinensky, A.M. Belcher, Label-free and high-resolution protein/DNA nanoarray analysis using Kelvin probe force microscopy, Nat. Nanotechnol. 2 (2007) 653–659, https://doi.org/10.1038/nnano.2007.293.
[19] H. Lee, W. Lee, J.H. Lee, D.S. Yoon, Surface potential analysis of nanoscale biomaterials and devices using Kelvin probe force microscopy, J. Nanomater. 2016 (2016), https://doi.org/10.1155/2016/4209130.
[20] Y. Yan, H. Yang, Y. Su, L. Qiao, Albumin adsorption on CoCrMo alloy surfaces, Sci. Rep. 5 (2015) 1–10, https://doi.org/10.1038/srep18403.
[21] E. Rahimi, R. Offoiach, K. Baert, H. Terryn, M. Lekka, L. Fedrizzi, Role of phosphate, calcium species and hydrogen peroxide on albumin protein adsorption on surface oxide of Ti6Al4V alloy, Materialia. 15 (2021), https://doi.org/10.1016/j.mtla.2020.100988.
[22] P.I. Harris, F. Severcan, eds., Vibrational Spectroscopy in Diagnosis and Screening (vol. 6), IOS Press, 2012. https://www.iospress.nl/book/vibrational-spectroscopy-in-diagnosis-and-screening/.
[23] L. Mandrile, G. Amato, D. Marchis, G. Martra, A.M. Rossi, Species-specific detection of processed animal proteins in feed by Raman spectroscopy, Food Chem. 229 (2017) 268–275, https://doi.org/10.1016/j.foodchem.2017.02.089.
[24] S. Schlücker, Surface-enhanced raman spectroscopy: Concepts and chemical applications, Angew. Chemie - Int. Ed. 53 (2014) 4756–4795, https://doi.org/10.1002/anie.201205748.
[25] L. Mandrile, A.M. Giovannozzi, F. Durbiano, G. Martra, A.M. Rossi, Rapid and sensitive detection of pyrimethanil residues on pome fruits by Surface Enhanced Raman Scattering, Food Chem. 244 (2018) 16–24, https://doi.org/10.1016/j.foodchem.2017.10.003.
[26] L. de Oliveira Noman, A.C. Sant'Ana, The control of the adsorption of bovine serum albumin on mercaptan-modified gold thin films investigated by SERS spectroscopy, Spectrochim. Acta - Part A Mol. Biomol. Spectrosc. 204 (2018) 119–124. 10.1016/j.saa.2018.06.030.
[27] N. Schwenk, B. Mizaikoff, S. Cárdenas, Á.I. López-Lorente, Gold-nanostar-based SERS substrates for studying protein aggregation processes, Analyst. 143 (2018) 5103–5111, https://doi.org/10.1039/C8AN00804C.
[28] A.S. Zhao, S. Zhou, Y. Wang, J. Chen, C.R. Ye, N. Huang, Molecular interaction of fibrinogen with thermally modified titanium dioxide nanoparticles, RSC Adv. 4 (2014) 40428–40434, https://doi.org/10.1039/c4ra07803a.
[29] J.A. Lee, W.K. Lee, Calcium phosphate-mediated surface modification of titanium oxide and its effects on surface potential and fibrinogen adsorption, J. Ind. Eng. Chem. 19 (2013) 1448–1456, https://doi.org/10.1016/j.jiec.2013.01.008.
[30] J.H. Adair, E. Suvaci, J. Sindel, Surface and Colloid Chemistry, in: Encycl. Mater. Sci. Technol., Elsevier, 2001: pp. 1–10. 10.1016/B0-08-043152-6/01622-3.
[31] S. Metwally, U. Stachewicz, Surface potential and charges impact on cell responses on biomaterials interfaces for medical applications, Mater. Sci. Eng. C. 104 (2019), https://doi.org/10.1016/j.msec.2019.109883 109883.
[32] S. Ferraris, M. Cazzola, V. Peretti, B. Stella, S. Spriano, Zeta potential measurements on solid surfaces for in Vitro biomaterials testing: Surface charge, reactivity upon contact with fluids and protein absorption, Front. Bioeng, Biotechnol. 6 (2018) 1–7, https://doi.org/10.3389/fbioe.2018.00060.
[33] L. Qian, P. Yu, J. Zeng, Z. Shi, Q. Wang, G. Tan, C. Ning, Large-scale functionalization of biomedical porous titanium scaffolds surface with TiO2 nanostructures医用多孔钛支架表面功能化二氧化钛纳米结构构建的研究, Sci. China Mater. 61 (4) (2018) 557–564.
[34] M. Oliveberg, V.L. Arcus, A.R. Fersht, pKA Values of Carboxyl Groups in the Native and Denatured States of Barnase: The pKA Values of the Denatured State Are on Average 0.4 Units Lower Than Those of Model Compounds, Biochemistry. 34 (1995) 9424–9433, https://doi.org/10.1021/bi00029a018.
[35] L. Mandrile, I. Cagnasso, L. Berta, A.M. Giovannozzi, M. Petrozziello, F. Pellegrino, A. Asproudi, F. Durbiano, A.M. Rossi, Direct quantification of sulfur dioxide in wine by Surface Enhanced Raman, Spectroscopy (2020), https://doi.org/10.1016/j.foodchem.2020.127009.
[36] S. Spriano, E. Verne, S. Ferraris, Multifunctional titanium surfaces for bone integration, EP 2 214 732 B1, 2007.
[37] S. Ferraris, S. Spriano, G. Pan, A. Venturello, C.L. Bianchi, R. Chiesa, M.G. Faga, G. Maina, E. Vernè, Surface modification of Ti–6Al–4V alloy for biomineralization and specific biological response: Part I, inorganic modification, J. Mater. Sci. Mater. Med. 22 (2011) 533–545, https://doi.org/10.1007/s10856-011-4246-2.
[38] H. Zeng, K.K. Chittur, W.R. Lacefield, Analysis of bovine serum albumin adsorption on calcium phosphate and titanium surfaces, Biomaterials. 20 (1999) 377–384, https://doi.org/10.1016/S0142-9612(98)00184-7.
[39] D. Nečas, P. Klapetek, Gwyddion: an open-source software for SPM data analysis, Open Phys. 10 (2012) 181–188, https://doi.org/10.2478/s11534-011-0096-2.
[40] S. Ferraris, S. Yamaguchi, N. Barbani, C. Cristallini, G. Gautier di Confiengo, J. Barberi, M. Cazzola, M. Miola, E. Vernè, S. Spriano, The mechanical and chemical stability of the interfaces in bioactive materials: The substrate-bioactive surface layer and hydroxyapatite-bioactive surface layer interfaces, Mater. Sci. Eng. C. 116 (2020), https://doi.org/10.1016/j.msec.2020.111238 111238.

[41] S. Yan, G.-L. Song, Z. Li, H. Wang, D. Zheng, F. Cao, M. Horynova, M.S. Dargusch, L. Zhou, A state-of-the-art review on passivation and biofouling of Ti and its alloys in marine environments, J. Mater. Sci. Technol. 34 (2018) 421–435, https://doi.org/10.1016/j.jmst.2017.11.021.
[42] D.-N. Le, H.T. Nguyen-Truong, Analytical Formula for the Electron Inelastic Mean Free Path, J. Phys. Chem. C. 125 (2021) 18946–18951, https://doi.org/10.1021/acs.jpcc.1c05212.
[43] G.G. Fuentes, E. Elizalde, F. Yubero, J.M. Sanz, Electron inelastic mean free path for Ti, TiC, TiN and TiO2 as determined by quantitative reflection electron energy-loss spectroscopy, Surf. Interface Anal. 33 (2002) 230–237, https://doi.org/10.1002/sia.1205.
[44] S.-H. Choi, J.-H. Ryu, J.-S. Kwon, J.-E. Kim, J.-Y. Cha, K.-J. Lee, H.-S. Yu, E.-H. Choi, K.-M. Kim, C.-J. Hwang, Effect of wet storage on the bioactivity of ultraviolet light- and non-thermal atmospheric pressure plasma-treated titanium and zirconia implant surfaces, Mater. Sci. Eng. C. 105 (2019), https://doi.org/10.1016/j.msec.2019.110049 110049.
[45] R.N. Foster, E.T. Harrison, D.G. Castner, ToF-SIMS and XPS Characterization of Protein Films Adsorbed onto Bare and Sodium Styrenesulfonate-Grafted Gold Substrates, Langmuir. 32 (2016) 3207–3216, https://doi.org/10.1021/acs.langmuir.5b04743.
[46] H. Lee, S.W. Lee, G. Lee, W. Lee, K. Nam, J.H. Lee, K.S. Hwang, J. Yang, H. Lee, S. Kim, S.W. Lee, D.S. Yoon, Identifying DNA mismatches at single-nucleotide resolution by probing individual surface potentials of DNA-capped nanoparticles, Nanoscale. 10 (2018) 538–547, https://doi.org/10.1039/C7NR05250B.
[47] K. Nam, K. Eom, J. Yang, J. Park, G. Lee, K. Jang, H. Lee, S.W. Lee, D.S. Yoon, C.Y. Lee, T. Kwon, Aptamer-functionalized nano-pattern based on carbon nanotube for sensitive, selective protein detection, J. Mater. Chem. 22 (2012) 23348–23356, https://doi.org/10.1039/c2jm33688j.
[48] I. Van De Keere, R. Willaert, A. Hubin, J. Vereecken, Interaction of human plasma fibrinogen with commercially pure titanium as studied with atomic force microscopy and X-ray photoelectron spectroscopy, Langmuir. 24 (2008) 1844–1852, https://doi.org/10.1021/la7016566.
[49] S. Kashiwaya, J. Morasch, V. Streibel, T. Toupance, W. Jaegermann, A. Klein, The Work Function of TiO2, Surfaces. 1 (2018) 73–89, https://doi.org/10.3390/surfaces1010007.
[50] E. Li-Chan, J.M. Chalmers, P.R. Griffiths (Eds.), Applications of Vibrational Spectroscopy in Food Science, John Wiley & Sons, 2010.
[51] L. Mandrile, M. Vona, A.M. Giovannozzi, J. Salafranca, G. Martra, A.M. Rossi, Migration study of organotin compounds from food packaging by surface-enhanced Raman scattering, Talanta. 220 (2020), https://doi.org/10.1016/j.talanta.2020.121408 121408.
[52] A. D'Agostino, A.M. Giovannozzi, L. Mandrile, A. Sacco, A.M. Rossi, A. Taglietti, In situ seed-growth synthesis of silver nanoplates on glass for the detection of food contaminants by surface enhanced Raman scattering, Talanta. 216 (2020), https://doi.org/10.1016/j.talanta.2020.120936 120936.
[53] G. Barzan, L. Rocchetti, C. Portesi, F. Pellegrino, A. Taglietti, A.M. Rossi, A.M. Giovannozzi, Surface Minimal Bactericidal Concentration: A comparative study of active glasses functionalized with different-sized silver nanoparticles, Colloids Surfaces B Biointerfaces. 204 (2021), https://doi.org/10.1016/j.colsurfb.2021.111800 111800.
[54] J.T. Pelton, L.R. McLean, Spectroscopic methods for analysis of protein secondary structure, Anal. Biochem. 277 (2000) 167–176, https://doi.org/10.1006/abio.1999.4320.
[55] Y. Kang, X. Li, Y. Tu, Q. Wang, H. Ågren, On the Mechanism of Protein Adsorption onto Hydroxylated and Nonhydroxylated TiO 2 Surfaces, J. Phys. Chem. C. 114 (2010) 14496–14502, https://doi.org/10.1021/jp1037156.
[56] F.Y. Oliva, L.B. Avalle, O.R. Cámara, C.P. De Pauli, Adsorption of human serum albumin (HSA) onto colloidal TiO2 particles, Part I, J. Colloid Interface Sci. 261 (2003) 299–311, https://doi.org/10.1016/S0021-9797(03)00029-8.
[57] S. Ferraris, S. Yamaguchi, N. Barbani, M. Cazzola, C. Cristallini, M. Miola, E. Vernè, S. Spriano, Bioactive materials: In vitro investigation of different mechanisms of hydroxyapatite precipitation, Acta Biomater. 102 (2019) 468–480, https://doi.org/10.1016/j.actbio.2019.11.024.
[58] S.E. Glassford, B. Byrne, S.G. Kazarian, Recent applications of ATR FTIR spectroscopy and imaging to proteins, Biochim. Biophys. Acta - Proteins Proteomics. 2013 (1834) 2849–2858, https://doi.org/10.1016/j.bbapap.2013.07.015.
[59] J. Shi, B. Feng, X. Lu, J. Weng, Adsorption of bovine serum albumin onto titanium dioxide nanotube arrays, Int. J. Mater. Res. 103 (2012) 889–896, https://doi.org/10.3139/146.110696.
[60] M. Xiao, M. Biao, Y. Chen, M. Xie, B. Yang, Regulating the osteogenic function of rhBMP 2 by different titanium surface properties, J. Biomed. Mater. Res. Part A. 104 (2016) 1882–1893, https://doi.org/10.1002/jbm.a.35719.
[61] X.J. Shi, D. Li, J. Xie, S. Wang, Z.Q. Wu, H. Chen, Spectroscopic investigation of the interactions between gold nanoparticles and bovine serum albumin, Chinese Sci. Bull. 57 (2012) 1109–1115, https://doi.org/10.1007/s11434-011-4741-3.
[62] Y. Li, Y. Bian, H. Qin, Y. Zhang, Z. Bian, Photocatalytic reduction behavior of hexavalent chromium on hydroxyl modified titanium dioxide, Appl. Catal. B Environ. 206 (2017) 293–299, https://doi.org/10.1016/j.apcatb.2017.01.044.
[63] B.S. Bal, M.N. Rahaman, Orthopedic applications of silicon nitride ceramics, Acta Biomater. 8 (2012) 2889–2898, https://doi.org/10.1016/j.actbio.2012.04.031.
[64] R. Li, Z. Wu, Y. Wangb, L. Ding, Y. Wang, Role of pH-induced structural change in protein aggregation in foam fractionation of bovine serum albumin, Biotechnol. Reports. 9 (2016) 46–52, https://doi.org/10.1016/j.btre.2016.01.002.
[65] T. Peters, All About Albumin, Elsevier (1995), https://doi.org/10.1016/B978-0-12-552110-9.X5000-4.
[66] S. Ravindran, M.A.K. Williams, R.L. Ward, G. Gillies, Understanding how the properties of whey protein stabilized emulsions depend on pH, ionic strength and calcium concentration, by mapping environmental conditions to zeta potential, Food Hydrocoll. 79 (2018) 572–578, https://doi.org/10.1016/j.foodhyd.2017.12.003.
[67] B. Meloun, L. Morávek, V. Kostka, Complete amino acid sequence of human serum albumin, FEBS Lett. 58 (1975) 134–137, https://doi.org/10.1016/0014-5793(75)80242-0.
[68] E. Migliorini, M. Weidenhaupt, C. Picart, Practical guide to characterize biomolecule adsorption on solid surfaces (Review), Biointerphases. 13 (2018) 06D303, https://doi.org/10.1116/1.5045122.